**Status report on modeling the Balbekov square ring in ICOOL**

**R.C. Fernow**
**17 December 2001**

We are in the process of setting up an ICOOL simulation of Valeri Balbekov's four-sided cooling ring [1] for the MUCOOL experiment, which is shown in Fig. 1. At present we are working with hard-edged models of the ring magnets. The ultimate goal is to develop a model with more realistic field profiles.

## 1. Problem geometry

The model consists of a 4-sided ring with circumference [1]

$$C = 36.955 \text{ m}$$

Each quadrant of the ring is identical. The geometric aspects of the elements are summarized in the following table.

| element | radius [m] | length [m] | Σ length [m] |
|---|---|---|---|
| drift | 0.60 | 0.072018 | 0.072 018 |
| RF1-8 | 0.57 | 8 × 0.32 | 2.632 018 |
| drift | 0.60 | 0.04 | 2.672 018 |
| LH2 | 0.31 | 1.334 | 4.006 018 |
| drift | 0.60 | 0.04 | 4.046 018 |
| RF9-16 | 0.57 | 8 × 0.32 | 6.606 018 |
| drift | 0.60 | 0.072018 | 6.678 036 |
| dipole | 0.52 | 0.408 407 | 7.086 443 |
| drift + wedge | 0.29 | 1.7439 | 8.830 343 |
| dipole | 0.52 | 0.408 407 | 9.238 750 |

## 2. Field modeling

COMBINED FUNCTION DIPOLE

The radius of the particle in the LAB is

$$r = \rho + x$$

where ρ is the radius of curvature and the transverse coordinates (x,y) are measured relative to the reference trajectory. On the magnet midplane the vertical field is

$$B_{yo} = B_D \sqrt{\frac{1}{1+\frac{x}{\rho}}}$$

and the horizontal field vanishes. Define

$$w = y / r$$

Off the midplane the field is given is given by the expansions [2]

$$B_Y = B_{yo}\left[1-\frac{1}{8}w^2+\frac{25}{384}w^4-\frac{45}{1024}w^6+\frac{7605}{229376}w^8\right]$$

and

$$B_X = -B_{yo}\frac{w}{2}SIGN(1,x)\left[1-\frac{5}{24}w^2+\frac{15}{128}w^4-\frac{585}{14336}w^6+\frac{14365}{458752}w^8\right]$$

The field is taken as uniform along the longitudinal direction and to end abruptly at the hard edge.

SOLENOIDS

The solenoids are modeled with current sheets. The relative current densities are taken from [1] and then multiplied by an adjustable scale factor to produce the desired field strength on-axis. The files include additional current sheets beyond the physical geometric region to simulate the effect of magnetic mirrors at the solenoid ends. The effect of the fringe fields at the ends of the solenoids are approximated by transverse momentum kicks that are proportional to the radius of the particle. The symmetry of the kick orientation repeats twice each turn. Starting with a long straight section we used the series {- + - - + - + +}.

## 3. Basic parameters

The ring contains 8 combined function dipoles with [1]

$B_D = 1.453$ T
$\rho = 0.52$ m
n = 1/2 (field index)

The dipole parameters fix the central momentum $p_o$ and related quantities

$p_o = 0.226\ 511\ 190$ GeV/c
$E_o = 0.249\ 942\ 008$ GeV
$KE_o = 0.144\ 283\ 651$ GeV
$\gamma_o = 2.365\ 567\ 81$
$\beta_o = 0.906\ 254\ 980$

The bend angle of $45^o$ fixes the arclength in the dipole

$s_D = 0.408\ 407\ 045$ m

The revolution time around the ring depends on the detailed momentum profile of the reference particle. Starting at $p_o$ the momentum will increase in the RF cavities in front of the hydrogen absorber, fall precipitously in the absorber, then increase again back to $p_o$ in the RF cavities after the absorber. However, we expect the average momentum over the whole path to be close to $p_o$ . In that case using

$m_\mu = 0.105\ 658\ 357$ GeV/c2
$c = 2.997\ 924\ 58\ 10^8$ m/s

we find that the revolution time is

$T_{REV} \approx 136.020$ ns

For the stated RF frequency of 201.25 MHz, the RF period is 4.9689 ns and the harmonic number is 27.37, not the integer value 28 given in [1].

## 4. Reference particle

ICOOL uses an internal reference particle to set the absolute phases of the RF cavities. The algorithm chosen starts with an on-axis particle with momentum $p_o$ and all stochastic processes turned off. The particle is tracked thru all regions except RF cavities. We took the length of liquid hydrogen absorber [1]

$$L_{ABS} = 1.334 \text{ m}$$

The particles loses 40.27 MeV in the absorber. This energy is made up in the 16 RF cavities in the straight section. The cavities are assumed to have pillbox fields with sinusoidally varying electric and magnetic fields and to have a length and peak on-axis gradient

$$L_{CAV} = 0.32 \text{ m}$$
$$G = 15 \text{ MV/m}$$

The phase algorithm assumes the reference particle gains energy at a constant rate while crossing each cavity. The parameter that specifies this rate

GRADREF = 7.865 179 082 MV/m

was adjusted so that the reference particle had momentum $p_o$ after leaving the 16th cavity. This fixes the reference particle trajectory. The time that the reference particle crosses the center of each cavity is determined and used to set the time that cavity is at zero-crossing of the electric field. With the appropriate parameters set to ~9 significant figures and using the double precision version of the code, the reference particle stayed on-axis for 15 complete turns, even without using the solenoid focusing. The final radial position error was ~0.2 μm and the transverse momentum error was ~5 $10^{-8}$ GeV/c.

We can use the reference particle trajectory to get a more accurate estimate of the revolution time. The upper left part of Fig. 2 shows the energy profile thru one quadrant of the ring. The rate of energy increase in the RF cavities is constant by design. The corresponding velocity profile is shown in the upper right part of the figure. This was used in a piecewise integration to obtain the accumulated time profile in the lower part of the figure. We find that the revolution time is

$$T_{REV} = 136.1341 \text{ ns}$$

Taking the harmonic number [1]

$$h = 28$$

The corresponding RF period and frequency is

$$T_{RF} = 4.8619 \text{ ns.}$$
$$f_{RF} = 205.6795 \text{ MHz}$$

## 5. Real on-axis, on-momentum particle

Now that the absolute cavity phases have been fixed we can look at tracking real particles. We assume that the cavities in the other three quadrants of the ring have the same absolute phase as the corresponding cavity in the first quadrant. We take a particle with momentum $p_o$. In order for the particle to get accelerated in the cavities we shift its launch time relative to the reference particle. By setting a parameter

T0REF = -0.473 248 92 ns

the particle phase crossing the cavities is just right to end up with momentum $p_o$ after leaving the 16th RF cavity. This corresponds to a synchronous phase of $35.0^o$.

However, there is a time shift of 8.8 ps between the real particle and the reference particle when leaving the 16th cavity. This means the real particle will enter the first cavity in the next quadrant at a different phase than it entered the first cavity in the first quadrant. Part of this time difference comes about because the real particle does not have the same momentum profile through the cavities and absorbers that was assumed for the reference particle. We attempted to reduce this error by setting an additional phase offset in each cavity in the first quadrant so that the momentum profile matched that of the reference particle. These phase offsets were small, the largest being $0.27^o$. However, the resultant time shift after the 16th cavity was only reduced to 7.8 ps with this procedure.

We showed that this time difference is small enough for multiturn tracking to work. A special run with the dipole fields set to 0 and no transverse focusing showed that the track successfully traversed a distance equivalent to 15 times the circumference, which in turn shows that this is a phase-stable solution.

With the dipole fields on and transverse focusing on, the real particle completed 15 turns around the ring. At the end the particle was ~0.03 mm off the axis and had a transverse momentum of ~0.01 MeV/c.

## 6. Transverse dynamics

Particles make ~5 betatron oscillations traversing the long straight section where the peak solenoid field is 5.17 T. The betatron wavelength is ~1.3 m.

## 7. Bend region

We checked the dispersion suppression in the design by looking at a simplified system consisting only of the dipole-short solenoid-dipole combination. For the first part of the study the wedge at the center of the solenoid was removed. On-axis particles were launched[1] with momenta near $p_o$. We adjusted the overall current density scale factor in order to minimize the transverse beam position and momentum at the end of the simplified system. This optimization was not straightforward since for some solutions the particles were subsequently lost in multiturn tracking. The dynamics of the ring seem to be strongly influenced by the exact design of this complicated field flip plus wedge region. The chosen solution produced a peak field of 2.72 T and a field at the solenoid hard edge of 2.064 T, in rough agreement with Fig. 3 in [1]. Adjusting the two coil current densities in the field flipping short solenoid independently did not improve the results.

We also used the dipole-short solenoid-dipole combination to check for proper operation of the LiH wedge. An on-axis beam was used with momentum spread $\sigma_{PZ}$ = 18 MeV/c. The beam is dispersed in x by the first dipole. The solenoidal field between the dipole and the wedge rotates the dispersion so that it lies mainly in the y direction going into the wedge. The wedge properties were [1]

$\alpha_W = 25.4^o$
width = 29 cm
thickness = 13.07 cm

The wedge is oriented vertically with the apex touching the beam axis. The effect of the wedge on the kinetic energy [MeV] of the beam is given in the table.

| | $y > 0$ | $y < 0$ |
|---|---|---|
| Before the wedge | 129.9 ± 10.9 | 158.9 ± 11.1 |
| After the wedge | 129.9 ± 10.9 | 156.5 ± 9.4 |

We see that, as desired, the average energy and the energy spread are reduced in one half of the vertical dimension and left alone in the other half.

The dispersion functions following the second dipole are shown in Figs. 3 and 4. The wedge was included in these simulations. The momentum region over which the displacement is small is ~10 MeV, limited mainly by the dispersion in x.

[1] For some unknown reason the multi-turn dynamics for the real ring were unstable if the scale factor was set to exactly correspond to $p_o$.

## 8. Ring behavior for off-momentum particles

Several properties of the ring can be determined from tracking particles with momentum unequal to $p_o$ through a single turn. The compaction factor is [3]

$$\alpha_p = \frac{\frac{\Delta C}{C}}{\frac{\Delta p}{p_o}}$$

The transition gamma is [3]

$$\gamma_t = \frac{1}{\sqrt{\alpha_p}}$$

The slip factor is [3]

$$\eta = \frac{1}{\gamma_t^2} - \frac{1}{\gamma_o^2}$$

We find

$\alpha_p = 1.223\ 10^{-3}$
$\gamma_t = 28.590$
$|\eta| = 0.177$

The longitudinal beta function is [4]

$$\beta_\phi^2 = \frac{1}{\beta^3 \gamma e V' \cos(\phi_s)} \frac{2\pi}{\lambda_{RF}} \frac{\eta}{mc^2}$$

where our synchronous phase is measured from zero-crossing. We find

$\beta_\phi = 0.0181\ \mathrm{MeV}^{-1}$

By observing the counter-clockwise rotation of the bunch in longitudinal phase space, we determined that the synchrotron wavelength is approximately the same as the circumference of the ring (~37 m).

An indication that the motion thru the wedges is not properly synchronized yet in the simulation can be seen in Fig. 5, which shows $p_Z$ for a particle that starts on-axis with p = 220 MeV/c. Although the particle is successfully tracked through 15 complete turns without being lost, the wedges do not damp the longitudinal momentum spread. The motion is regular for the first ~5 turns, after which the amplitude of the oscillations increase significantly. Similar behavior is seen for a particle starting at 233 MeV/c.

## 9. Initial beam conditions

We assume the initial beam parameters were [1]

$\sigma_X = \sigma_Y = 4$ cm
$\sigma_{PX} = \sigma_{PY} = 32$ MeV/c
$\sigma_Z = 8.9$ cm
$\sigma_{PZ} = 18$ MeV/c (without correlation)

The initial beam was given a transverse amplitude-momentum correlation according to the following prescription [5]. Let us define the Balbekov amplitude

$$A_B = \frac{p_o}{m_\mu c}\sqrt{\left(\frac{r}{\beta_\perp}\right)^2 + (x')^2 + (y')^2}$$

The quantities {r, x', y'} are randomly chosen to determine the initial value of this amplitude. The quantity $\beta_\perp$ is fixed at 30 cm, as in [1]. Once $A_B$ is known, we set the total energy of the particle according to

$$E = E_{REF}\sqrt{1 + A_B^{\;2}} + \Delta E$$

The quantity $E_{REF}$ is fixed at 250 MeV, as in [1], and $\Delta E$ was selected randomly. Fig. 6 shows the resulting correlation of total energy versus the Balbekov amplitude when $\Delta E=0$.

## 10. Full beam simulations

We are just beginning to look at gaussian beam simulations. Stochastic effects are still neglected. We first looked at the beam injected after a dipole and before a long straight section. The energy-amplitude correlation was applied to the beam. The transmission after one turn was 70%. Fig. 7 shows the longitudinal phase space after one turn. The major problem seems to be particles falling out of the RF bucket.

## Notes and references

[1] V. Balbekov et al, Muon ring cooler for the MUCOOL experiment, Proc. PAC 2001.
[2] The coefficients of these expansions were taken from the Geant parameter file mucool.rcp in Oct. 2001.
[3] A. Chao & M. Tigner, Handbook of Accelerator Physics and Engineering, World Scientific, 1999, p. 50-1.
[4] D. Neuffer, Calculations of predicted performance for μ-cooling rings, MC note 227, 2001.
[5] V. Balbekov, private communication, 12 December 2001.

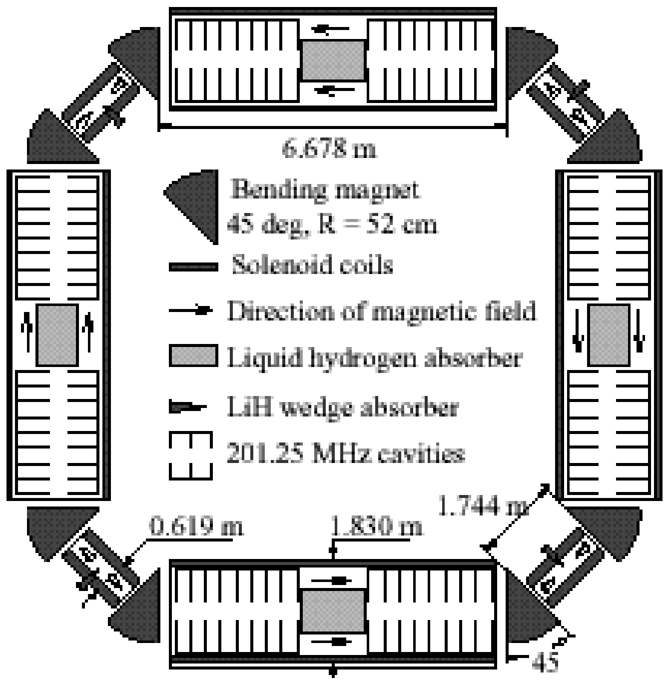


Figure 1: Layout of the ring cooler.

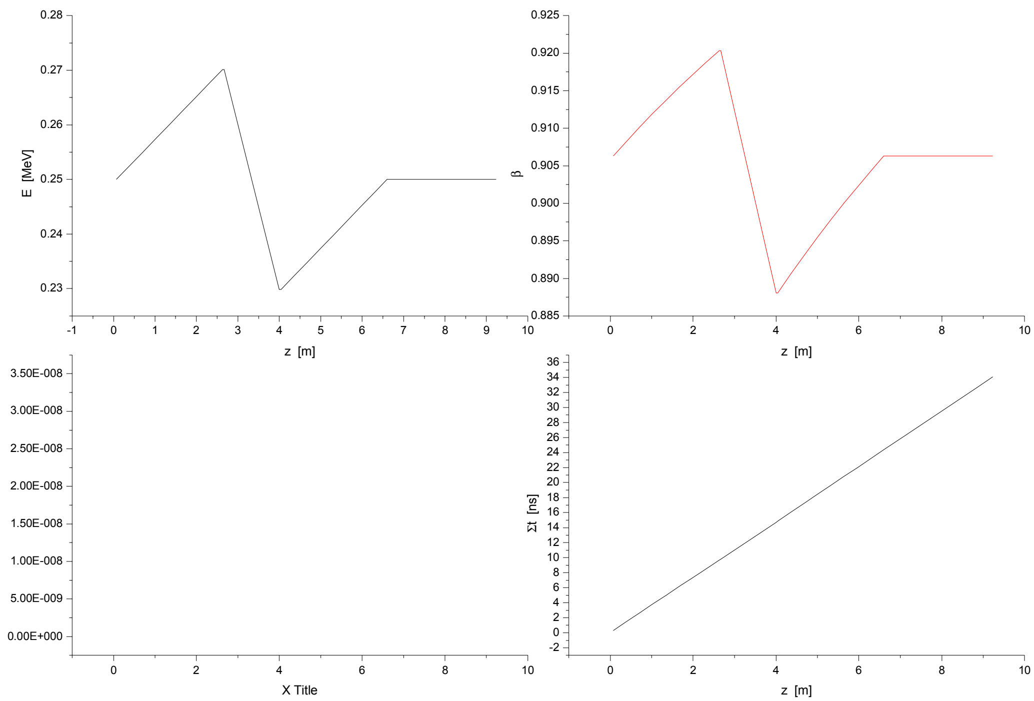


**Figure 2** Energy and velocity profiles and accumulated time for reference particle through one quadrant of the ring.

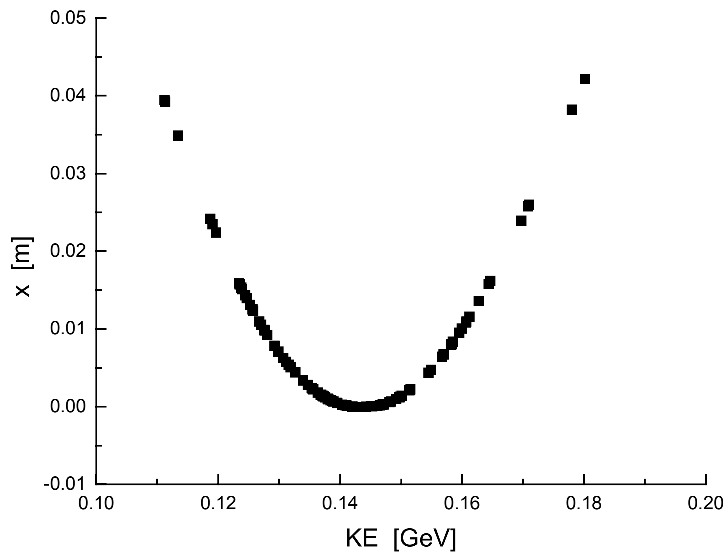


**Figure 3** Horizontal dispersion after the second dipole.

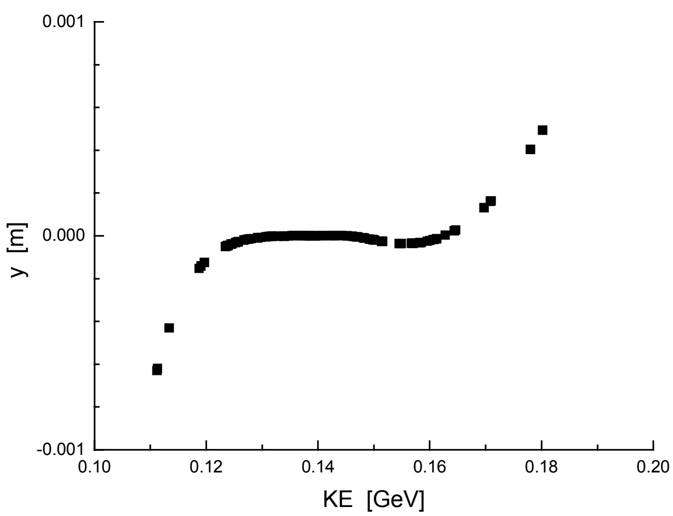


**Figure 4** Vertical dispersion after the second dipole.

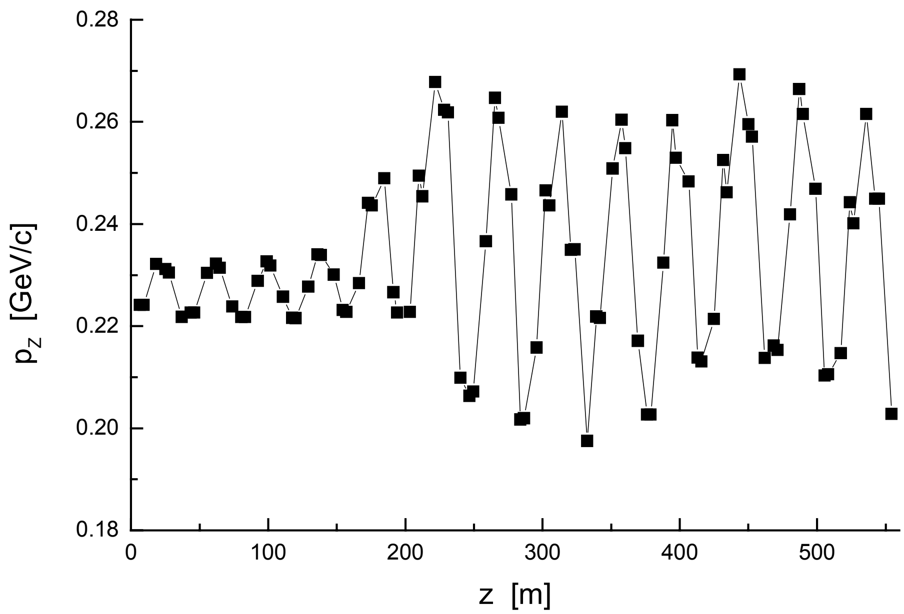


**Figure 5** Longitudinal momentum for a track starting on-axis with p = 220 MeV/c.

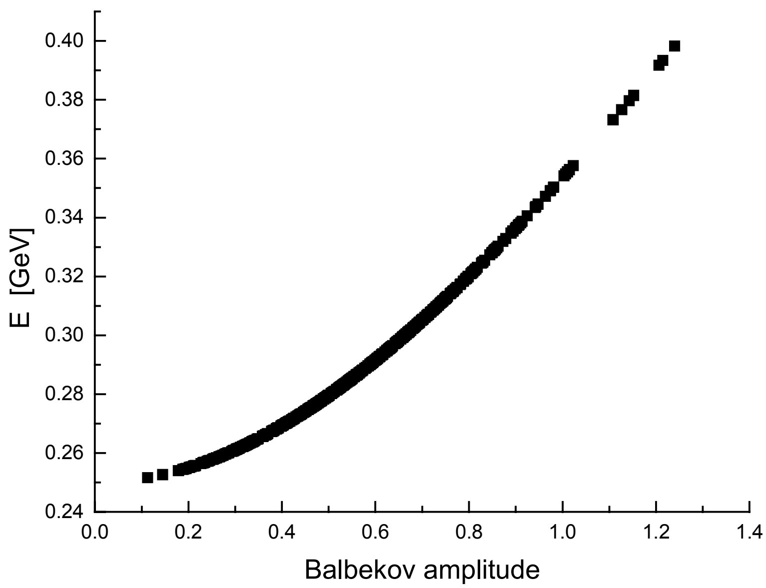


**Figure 6** Initial value of the total energy as a function of the Balbekov amplitude

.

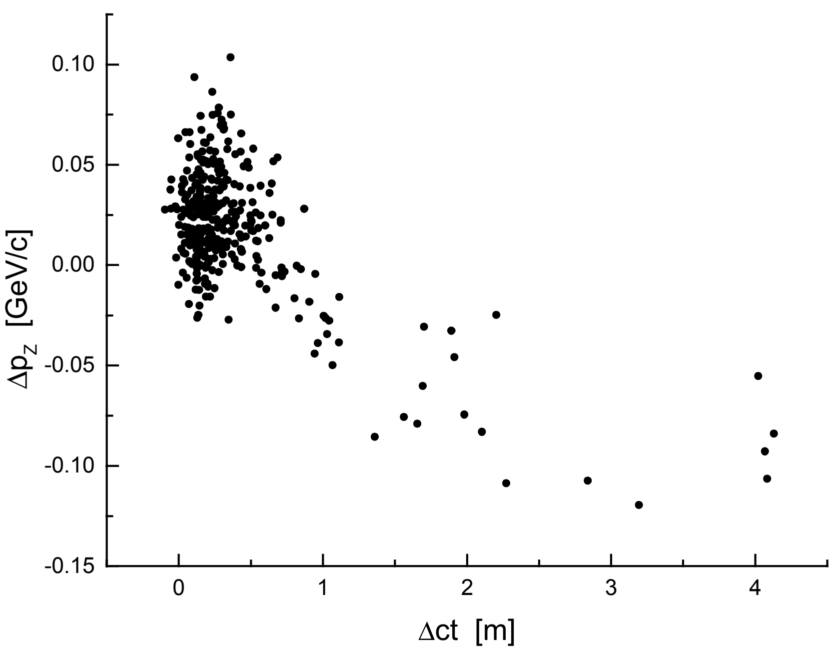


**Figure 7** Longitudinal phase space after one turn.